Bull. Korean Math. Soc. **61** (2024), No. 1, pp. 93–115
https://doi.org/10.4134/BKMS.b230051
pISSN: 1015-8634 / eISSN: 2234-3016

UNCONDITIONALLY STABLE GAUGE-UZAWA FINITE ELEMENT METHODS FOR THE DARCY-BRINKMAN EQUATIONS DRIVEN BY TEMPERATURE AND SALT CONCENTRATION

Yangwei Liao and Demin Liu

Abstract. In this paper, the Gauge-Uzawa methods for the Darcy-Brinkman equations driven by temperature and salt concentration (DBTC) are proposed. The first order backward difference formula is adopted to approximate the time derivative term, and the linear term is treated implicitly, the nonlinear terms are treated semi-implicit. In each time step, the coupling elliptic problems of velocity, temperature and salt concentration are solved, and then the pressure is solved. The unconditional stability and error estimations of the first order semi-discrete scheme are derived, at the same time, the unconditional stability of the first order fully discrete scheme is obtained. Some numerical experiments verify the theoretical prediction and show the effectiveness of the proposed methods.

1. Introduction

The DBTC can be used to describe the double-diffusive convection phenomenon driven by temperature and salt concentration, where the salt concentration changes with temperature [5, 18, 21, 24]. The DBTC have a wide variety of applications such as metallurgy, grain storage and contaminant transport in ground water [1]. So the equations play a key role in industry and engineering today.

Due to the DBTC have important applications in industry production, a lot of researches for the Darcy-Brinkman equations, in which salt concentration is not affected by temperature, have been done in the past decades. In the fields of theoretical analysis, according to the fixed point theorem in the Banach space, Zhu et al. [26] proved that if the body forces belong to appropriate Sobolev

Received January 31, 2023; Revised March 19, 2023; Accepted March 30, 2023.
2020 *Mathematics Subject Classification.* Primary 65Mxx, 35Qxx, 76Dxx, 76Mxx.
Key words and phrases. Darcy-Brinkman equations, Gauge-Uzawa, finite element method, incompressible flow.
Research Fund from the Key Laboratory of Xinjiang Province (No.2022D04014); National Natural Science Foundation of China (No.12061075); Xinjiang Key Laboratory of Applied Mathematics (No.XJDX1401).

spaces, the stationary Darcy-Brinkman equations possess a unique weak solution. Liu [9] studied the structural stability for Brinkman-Forchheimer equations which can be seen as an extension of the Darcy-Brinkman equations, and proved the convergence and continuous dependence results about the Darcy coefficient λ. Tone et al. [21] proposed a second order scheme for the Darcy-Brinkman equations with the Darcy coefficient $\lambda = 0$ which based on backward differentiation formula for the time derivative and explicitly for the nonlinear term, proved the existence of attractors. In the fields of numerical simulation, Goyeau et al. [5] proposed the finite volume method for the Darcy-Brinkman equations. Applying the Fourier-Galerkin spectral method to the Darcy-Brinkman equations, Shao et al. [18] obtained the high-precision solution in confined saturated porous media. Çıbık et al. [2] proposed and analyzed a family of second order time stepping methods for the Darcy-Brinkman equations. Yang and Jiang [24] proposed a fully explicitly uncoupled variational multiscale stabilization method for the Darcy-Brinkman equations, they added a separate, uncoupled, and modular postprocessing step to each time step. Zeng et al. [25] proposed the deferred defect-correction method for the Darcy-Brinkman equations based on the mixed finite element method and deduced unconditional stability and convergence of the method. Liao and Huang [8] investigated the modified characteristics method for the Darcy-Brinkman equations, and so on.

It is noted that there are some numerical difficulties for the DBTC: (i) multiphysics field; (ii) the coupling of the velocity and pressure through the incompressibility constraint; (iii) nonlinear properties, which make the equations difficult to be solved numerically. So it is still a challenging to construct a stable and efficient numerical method for the DBTC. The above mentioned methods still need to solve the saddle-point problem, which results in the large-scale coupled system, so the above mentioned methods need to satisfy LBB condition. Recently, the Gauge-Uzawa method was widely used to approximate the Navier-Stokes equations, which can increase the stability of numerical solution, reduce the solution scale and improve the computational efficiency. Pyo [14] proposed the semi-discrete Gauge-Uzawa method for the Navier-Stokes equations, and the optimal error estimate was obtained by the energy method. Pyo and Shen [15] designed the second order time discretization scheme of Navier-Stokes equations through the second order backward difference formula. In addition, Pyo and Shen [16] extended the Gauge-Uzawa method to solve the Navier-Stokes equations with variable density. Feng et al. [23] applied the Gauge-Uzawa method to the natural convection equations with variable density, some numerical experiments were given to illustrate the effectiveness of the method.

Inspired by Nochetto and Pyo [11, 12], the Gauge-Uzawa methods for the DBTC are proposed in this paper. The basic idea of the methods is that backward difference formulas are used to approximate the time derivative term,

and the linear term is treated implicitly, the nonlinear terms are treated semi-implicit, which can reduce the scale of calculation and save costs. Moreover, the unconditional stability of the first order semi-discrete and full discrete scheme are deduced, and the error estimations of the first order semi-discrete scheme are derived. Some numerical experiments verify the theoretical prediction and show the effectiveness of the proposed method.

The remainder of this paper is organized as follows. In Section 2, the DBTC and preliminaries are given. In Section 3, the first order semi-discrete Gauge-Uzawa method is given, and the stability and error estimations of the first order semi-discrete method are deduced. In Section 4, the first order full discretization method is presented, and the stability of the first order full discretization method is deduced. In Section 5, numerical experiments are showed to confirm theoretical results.

2. Problem statement and variational formulation

2.1. Problem statement

In this paper, let $\Omega \subset R^d$, $d = 2$ or 3, be a connected domain with sufficiently smooth boundary $\partial\Omega$. For all $(x,t) \in \Omega \times (0, \mathcal{T}]$, the dimensionless form of the DBTC can be written as:

$$
(1) \qquad \begin{cases} u_t - \nu\Delta u + (u\cdot\nabla)u + \lambda u + \nabla p = f + R_a T g - R_s C g, \\ \nabla \cdot u = 0, \\ T_t + (u\cdot\nabla)T - \Delta T = \gamma, \\ C_t + (u\cdot\nabla)C - \Delta C = \eta + \mathcal{L}\Psi(T) - \kappa C, \end{cases}
$$

where the unknown variables are velocity $u = u(x,t)$, pressure $p = p(x,t)$, temperature $T = T(x,t)$ and salt concentration $C = C(x,t)$. The coupling system of (1) represents the conservation laws of momentum, mass, energy and salt concentration. The other constants R_a, R_s are the thermal and solutal Rayleigh numbers, $\mathcal{L} \geq 0$ is the chemical equilibrium coefficient, $\kappa \geq 0$ is the salt concentration coefficient. Besides, the parameter $\nu > 0$ is the kinematic viscosity, λ is the Darcy coefficient, g represents the gravitational acceleration, f is the body forces, γ and η denote the source terms [4]. The function Ψ is at least $\mathcal{C}^1$, and $\mathcal{L}\Psi(T)$ is considered to be the chemical equilibrium term. Based on [10, 13, 22], $\mathcal{L}\Psi(T) = \mathcal{L}T$ is assumed in this paper. Furthermore, the homogeneous Dirichlet boundary conditions

$$
(2) \qquad u = 0, \quad T = 0, \quad C = 0,
$$

and the initial conditions

$$
(3) \qquad u(x,0) = u^0(x), \quad T(x,0) = T^0(x), \quad C(x,0) = C^0(x),
$$

are supplied for (1).

2.2. Variational formulation

Let $H^m(\Omega)$, $m = 0, 1, 2, \ldots$, denote the Sobolev spaces, equipped with the norm $\|\cdot\|_m$, and $H_0^m(\Omega)$ denote the subspace of $H^m(\Omega)$ with the homogeneous boundary conditions. In particular, when $m = 0$, let $H^0(\Omega) = L^2(\Omega)$ denote the square integrable Sobolev space equipped with inner product $(\cdot, \cdot)$ and norm $\|\cdot\|_0$. Furthermore, let $H^{-1}(\Omega)$ is the dual space of $H_0^1(\Omega)$ equipped with norm

$$\|f\|_{-1} = \sup_{v \in H_0^1(\Omega)} \frac{|(f, v)|}{\|\nabla v\|_0}, \qquad \forall f \in H^{-1}(\Omega).$$

In order to consider the variational problem of (1), the following Sobolev spaces are introduced.

$$\begin{aligned}
&X = H_0^1(\Omega)^d, \quad M = H_0^1(\Omega),\\
&Y = L_0^2(\Omega) = \Big\{ v \in L^2(\Omega) : \int_\Omega q(x)\mathrm{d}x = 0 \Big\},\\
&V = \Big\{ v \in X : \nabla \cdot v = 0 \Big\},\\
&H = \Big\{ v \in X : \nabla \cdot v = 0,\ v \cdot n|_{\partial\Omega} = 0 \Big\}.
\end{aligned}$$

The Galerkin variational problem of (1) is: for all $t \in (0, \mathcal{T}]$, find $(u, p, T, C) \in X \times Y \times M \times M$, such that for all $(v, q, W, S) \in X \times Y \times M \times M$, there exists

$$(4) \quad \begin{cases}
(u_t, v) + \nu a(u, v) + b_1(u, u, v) + \lambda(u, v) = (f, v) + R_a(Tg, v) - R_s(Cg, v),\\
d(u, q) = 0,\\
(T_t, W) + \widetilde{a}(T, W) + b_2(u, T, W) = (\gamma, W),\\
(C_t, S) + \widetilde{a}(C, S) + b_2(u, C, S) = (\eta, S) + (\mathcal{L}\Psi(T), S) - (\kappa C, S),
\end{cases}$$

where the bilinear and trilinear forms are defined as follows:

$$\begin{aligned}
&a(u, v) = (\nabla u, \nabla v), \quad \tilde{a}(T, W) = (\nabla T, \nabla W),\\
&d(v, p) = (\nabla \cdot v, q),\\
&b_1(u, u, v) = \frac{1}{2}((u \cdot \nabla)u, v) - \frac{1}{2}((u \cdot \nabla)v, u),\\
&b_2(u, T, W) = \frac{1}{2}((u \cdot \nabla)T, W) - \frac{1}{2}(u \cdot \nabla)W, T).
\end{aligned}$$

The following properties of $b_1(\cdot, \cdot, \cdot)$ are well known [20]:

$$b_1(u, v, w) = -b_1(u, w, v), \quad b_1(u, v, v) = 0, \quad \forall u \in H, \quad \forall w, v \in X,$$

and

$$b_1(u, v, w) \le \begin{cases}
c\|u\|_1\|v\|_1\|w\|_1, & \forall u, v, w \in X,\\
c\|u\|_2\|v\|_0\|w\|_1, & \forall u \in H^2(\Omega)^d \cap X, \quad \forall v, w \in X,\\
c\|u\|_2\|v\|_1\|w\|_0, & \forall u \in H^2(\Omega)^d \cap X, \quad \forall v, w \in X,\\
c\|u\|_1\|v\|_2\|w\|_0, & \forall v \in H^2(\Omega)^d \cap X, \quad \forall u, w \in X.
\end{cases}$$

For simplicity, in the following paragraph, c is used to denote a general positive constant which depends on Ω, f, s, h, u^0, T^0, C^0, and other constants from various Sobolev inequalities.

Based on Hölder inequality, Poincaré inequality and Sobolev imbedding theorems, it is easy to prove that $b_2(\cdot,\cdot,\cdot)$ satisfies the following properties [17]:

$$b_2(u,T,W) = -b_2(u,W,T), \quad b_2(u,T,T) = 0, \quad \forall u \in H, \quad \forall T, W \in M,$$

and

$$b_2(u,T,W) \le \begin{cases} c\|u\|_1\|T\|_1\|W\|_1, & \forall u,T,W \in X, \quad \forall T,W \in M, \\ c\|u\|_2\|T\|_0\|W\|_1, & \forall u \in H^2(\Omega)^d \cap X, \quad \forall T,W \in M, \\ c\|u\|_2\|T\|_1\|W\|_0, & \forall u \in H^2(\Omega)^d \cap X, \quad \forall T,W \in M, \\ c\|u\|_1\|T\|_2\|W\|_0, & \forall T \in H^2(\Omega)^d \cap X, \quad \forall u \in X, \forall W \in M. \end{cases}$$

In order to consider the regularity and error estimations of the numerical solution, there still need to introduce some regularity assumptions about initial conditions, the right-hand terms and weak solutions.

Assumption 1. Suppose the initial conditions and the right-hand terms satisfies the regularity:

$$\begin{cases} u^0 \in H^2(\Omega)^d \cap V, \quad T^0,\ C^0 \in H^2(\Omega) \cap X, \\ f,\gamma,\eta \in L^\infty(0,\mathcal{T};L^2(\Omega)^d) \cap L^2(0,\mathcal{T};H^1(\Omega)^d). \end{cases} \tag{5}$$

Based on the general energy technique and the argument of regularity property of solution [20], the following regularity assumption is reasonable.

Assumption 2. Let $(u(t),p(t),T(t),C(t))$ be the week solution of (4). Then there exists some positive constant $\mathcal{M}$ such that the solution of (1) satisfies:

$$\begin{cases} \sup\limits_{t\in[0,\mathcal{T}]} \big\{\|u(t)\|_2 + \|T(t)\|_2 + \|C(t)\|_2 \\ +\|u_t(t)\|_0 + \|T_t(t)\|_0 + \|C_t(t)\|_0 + \|p(t)\|_0\big\} \le \mathcal{M}, \\ \displaystyle\int_0^{\mathcal{T}} \|\nabla u_t(t)\|_0^2 \mathrm{d}t + \int_0^{\mathcal{T}} \|\nabla T_t(t)\|_0^2 \mathrm{d}t + \int_0^{\mathcal{T}} \|\nabla C_t(t)\|_0^2 \mathrm{d}t \le \mathcal{M}, \\ \displaystyle\int_0^{\mathcal{T}} \|u_{tt}(t)\|_{-1}^2 \mathrm{d}t + \int_0^{\mathcal{T}} \|T_{tt}(t)\|_{-1}^2 \mathrm{d}t + \int_0^{\mathcal{T}} \|C_{tt}(t)\|_{-1}^2 \mathrm{d}t \le \mathcal{M}. \end{cases} \tag{6}$$

Next, let present the following discrete Gronwall's inequality [19].

Lemma 2.1. *Let $\{y^n\}$, $\{h^n\}$, $\{g^n\}$, $\{f^n\}$ be nonnegative time dependent sequences satisfying. B and C_* are given constants, $\forall m = 1,2,\ldots,\mathcal{N} = [\frac{\mathcal{T}}{\tau}]$,*

$$y^m + \tau\sum_{n=0}^{m} h^n \le B + \tau\sum_{n=0}^{m}(g^n y^n + f^n), \ \textit{with} \ \sum_{n=0}^{N} g^n \le C_*.$$

Assume $\tau g^n < 1$ and let $\sigma = \max\limits_{0\le n\le\mathcal{N}}(1-\tau g^n)^{-1}$. Then there exist:

$$y^m + \tau\sum_{n=0}^{m} h^n \le \exp(\sigma M)\big(B + \tau\sum_{n=0}^{m} f^n\big), \quad \forall m \le \mathcal{N}.$$

3. Semi-discrete Gauge-Uzawa scheme

The first order semi-discrete Gauge-Uzawa method can be listed as:

Algorithm 1: Suppose u^0, T^0 and C^0 are given and let $s^0 = 0$, assume that u^n, T^n and C^n are known. Then find $\widetilde{u}^{n+1}$, u^{n+1}, p^{n+1}, T^{n+1}, C^{n+1} from the following steps:

Step 1. Find $\widetilde{u}^{n+1}$, T^{n+1}, C^{n+1} as the solution of

$$
\begin{cases}
\frac{\widetilde{u}^{n+1}-u^n}{\tau} - \nu\Delta\widetilde{u}^{n+1} + (u^n\cdot\nabla)\widetilde{u}^{n+1} + \lambda\widetilde{u}^{n+1} + \nu\nabla s^n \\
= f^{n+1} + R_a g T^{n+1} - R_s g C^{n+1}, \\
\frac{T^{n+1}-T^n}{\tau} - \Delta T^{n+1} + (u^n\cdot\nabla)T^{n+1} = \gamma^{n+1}, \\
\frac{C^{n+1}-C^n}{\tau} - \Delta C^{n+1} + (u^n\cdot\nabla)C^{n+1} = \eta^{n+1} + \mathcal{L}\Psi(T^{n+1}) - \kappa C^{n+1}, \\
\widetilde{u}^{n+1}|_{\partial\Omega} = 0, \quad T^{n+1}|_{\partial\Omega} = 0, \quad C^{n+1}|_{\partial\Omega} = 0,
\end{cases} \tag{7}
$$

where

$$
f^{n+1} = \frac{1}{\tau}\int_{t_n}^{t_{n+1}} f(t)\mathrm{d}t, \quad \gamma^{n+1} = \frac{1}{\tau}\int_{t_n}^{t_{n+1}} \gamma(t)\mathrm{d}t, \quad \eta^{n+1} = \frac{1}{\tau}\int_{t_n}^{t_{n+1}} \eta(t)\mathrm{d}t.
$$

Step 2. Find ρ^{n+1} as the solution of

$$
\begin{cases}
-\Delta\rho^{n+1} = \nabla\cdot\widetilde{u}^{n+1}, \\
\partial_n\rho^{n+1}|_{\partial\Omega} = 0.
\end{cases} \tag{8}
$$

Step 3. Update u^{n+1} and s^{n+1} by

$$
\begin{cases}
u^{n+1} = \widetilde{u}^{n+1} + \nabla\rho^{n+1}, \\
s^{n+1} = s^n - \nabla\cdot\widetilde{u}^{n+1}.
\end{cases} \tag{9}
$$

Remark 3.1. $\widetilde{u}^{n+1}$ is eliminated from the first equation of (7) by using (9) and $\nabla\cdot u^{n+1} = 0$, $u^{n+1}\cdot n|_{\partial\Omega} = 0$, so pressure approximation can be updated by using the following formula

$$
p^{n+1} = -\frac{1}{\tau}\rho^{n+1} + \nu s^{n+1}. \tag{10}
$$

3.1. Stability and error analysis

Next, stability analysis of velocities, temperature and salt concentration for Algorithm 1 are derived.

3.1.1. *Stability.*

Theorem 3.2. *For all $1 \le N \le \mathcal{N}-1$, the numerical solution of Algorithm 1 is unconditionally stable*

$$
\begin{aligned}
&\|\widetilde{u}^N\|_0^2 + \|T^N\|_0^2 + \|C^N\|_0^2 + \nu\tau\|s^N\|_0^2 \\
&+ \sum_{n=0}^{N-1}(\|\widetilde{u}^{n+1}-u^n\|_0^2 + \|T^{n+1}-T^n\|_0^2 + \|C^{n+1}-C^n\|_0^2)
\end{aligned} \tag{11}
$$

$$
\begin{aligned}
&+\tau\sum_{n=0}^{N-1}(\nu\|\nabla\widetilde{u}^{n+1}\|_0^2+\|\nabla T^{n+1}\|_0^2+\|\nabla C^{n+1}\|_0^2)\\
\le\ &\|\widetilde{u}^0\|_0^2+\|T^0\|_0^2+\|C^0\|_0^2+\nu\tau\|s^0\|_0^2\\
&+c\int_0^{\mathcal{T}}(\|f(t)\|_0^2+\|\gamma(t)\|_0^2+\|\eta(t)\|_0^2)\mathrm{d}t+c\tau\mathcal{L}.
\end{aligned}
$$

Proof. Taking the inner product of (7) with $2\tau\widetilde{u}^{n+1}$, $2\tau T^{n+1}$ and $2\tau C^{n+1}$ to have

$$
\begin{cases}
\|T^{n+1}\|_0^2-\|T^n\|_0^2+\|T^{n+1}-T^n\|_0^2+2\tau\|\nabla T^{n+1}\|_0^2\\
=2\tau(\gamma^{n+1},T^{n+1})\le 2\tau\|T^{n+1}\|_0\|\gamma^{n+1}\|_0\\
\qquad\qquad\le\dfrac{\tau}{2}\|\nabla T^{n+1}\|_0^2+c\displaystyle\int_{t_n}^{t_{n+1}}\|\gamma(t)\|_0^2\mathrm{d}t,\\
\|C^{n+1}\|_0^2-\|C^n\|_0^2+\|C^{n+1}-C^n\|_0^2+2\tau\|\nabla C^{n+1}\|_0^2+2\kappa\tau\|C^{n+1}\|_0^2\\
=2\tau(\eta^{n+1},C^{n+1})+2\tau(\mathcal{L}\Psi(T^{n+1}),C^{n+1})\\
\le\dfrac{\tau}{2}\|\nabla C^{n+1}\|_0^2+c\tau\mathcal{L}+c\displaystyle\int_{t_n}^{t_{n+1}}\|\eta(t)\|_0^2\mathrm{d}t,
\end{cases}
\tag{12}
$$

$$
\begin{aligned}
&\|\widetilde{u}^{n+1}\|_0^2-\|u^n\|_0^2+\|\widetilde{u}^{n+1}-u^n\|_0^2\\
&+2\tau\|\nabla\widetilde{u}^{n+1}\|_0^2+2\tau\lambda\|\widetilde{u}^{n+1}\|_0^2+2\tau(\nabla s^n,\widetilde{u}^{n+1})\\
=\ &2\tau(f^{n+1},\widetilde{u}^{n+1})+2\tau R_a g(T^{n+1},\widetilde{u}^{n+1})-2\tau R_s g(C^{n+1},\widetilde{u}^{n+1}).
\end{aligned}
\tag{13}
$$

It can be derived from (8) that

$$
\begin{aligned}
\|u^n\|_0^2&=(u^n,u^n)\\
&=(\widetilde{u}^n+\nabla\rho^n,u^n)\\
&=(\widetilde{u}^n,u^n)\\
&=(\widetilde{u}^n,\widetilde{u}^n+\nabla\rho^n)=\|\widetilde{u}^n\|_0^2-\|\nabla\rho^n\|_0^2.
\end{aligned}
\tag{14}
$$

Due to (13), it can be deduced that

$$
\begin{aligned}
&\|\widetilde{u}^{n+1}\|_0^2-\|\widetilde{u}^n\|_0^2+\|\widetilde{u}^{n+1}-u^n\|_0^2+2\tau\|\nabla\widetilde{u}^{n+1}\|_0^2+2\tau\lambda\|\widetilde{u}^{n+1}\|_0^2\\
&+\|\nabla\rho^n\|_0^2\\
=\ &2\tau(f^{n+1},\widetilde{u}^{n+1})+2\tau R_a g(T^{n+1},\widetilde{u}^{n+1})-2\tau R_s g(C^{n+1},\widetilde{u}^{n+1})\\
&+2\tau(s^n,\nabla\cdot\widetilde{u}^{n+1})\\
=\ &\sum_{n=1}^{4}A_i.
\end{aligned}
\tag{15}
$$

From the Cauchy-Schwarz inequality and (9), it can be derived that

$$
\begin{cases}
A_1 = 2\nu\tau(s^n, s^{n+1}-s^n) = -\nu\tau(\|s^{n+1}\|_0^2 - \|s^n - s^{n+1}\|_0^2 - \|s^n\|_0^2) \\
\quad \le -\nu\tau(\|s^{n+1}\|_0^2 - \|s^n\|_0^2) + \nu\tau\|\nabla\widetilde{u}^{n+1}\|_0^2, \\
A_2 = 2\tau(f^{n+1}, \widetilde{u}^{n+1}) \le 2\tau\|f^{n+1}\|_0\|\widetilde{u}^{n+1}\|_0 \\
\quad \le \dfrac{\nu\tau}{4}\|\widetilde{u}^{n+1}\|_0^2 + c\displaystyle\int_{t_n}^{t_{n+1}} \|f(t)\|_0^2 \mathrm{d}t, \\
A_3 \le 2\tau R_a g|(T^{n+1}, \widetilde{u}^{n+1})| \le \dfrac{\nu\tau}{4}\|\widetilde{u}^{n+1}\|_0^2 + \dfrac{\tau}{2}\|\nabla T^{n+1}\|_0^2, \\
A_4 \le 2\tau R_s g|(C^{n+1}, \widetilde{u}^{n+1})| \le \dfrac{\nu\tau}{4}\|\widetilde{u}^{n+1}\|_0^2 + \dfrac{\tau}{2}\|\nabla C^{n+1}\|_0^2.
\end{cases} \tag{16}
$$

Adding up (12), (13) and (15) for $n = 0, 1, \ldots, N-1$, noting that (14) the proof is finished. □

3.1.2. *Error analysis.* Now let prove the optimal error estimates of presented method. In order to simplify the descriptions, let introduce the error symbols:

$$
\begin{aligned}
&e_u^{n+1} = u(t_{n+1}) - u^{n+1}, \quad \widetilde{e}_u^{n+1} = u(t_{n+1}) - \widetilde{u}^{n+1}, \\
&e_C^{n+1} = C(t_{n+1}) - C^{n+1}, \quad e_T^{n+1} = T(t_{n+1}) - T^{n+1}.
\end{aligned}
$$

Theorem 3.3. *Suppose Assumptions 1 and Assumptions 2 hold. Then, for all* $1 \le N \le \mathcal{N} - 1$, *there exists*

$$
\begin{aligned}
&\|e_u^N\|_0^2 + \|e_T^N\|_0^2 + \|e_C^N\|_0^2 \\
&+ \sum_{n=0}^{N-1}(\|\widetilde{e}_u^{n+1} - e_u^n\|_0^2 + \|e_T^{n+1} - e_T^n\|_0^2 + \|e_C^{n+1} - e_C^n\|_0^2) \\
&+ \tau\sum_{n=0}^{N-1}(\nu\|\nabla\widetilde{e}_u^{n+1}\|_0^2 + \|\nabla e_T^{n+1}\|_0^2 + \|\nabla e_C^{n+1}\|_0^2) \le c\tau^2.
\end{aligned} \tag{17}
$$

Proof. By expanding the exact solutions $u(t)$, $T(t)$, $C(t)$ through Taylor formulas, it can be obtained

$$
\begin{aligned}
&\frac{u(t_{n+1}) - u(t_n)}{\tau} - \nu\Delta u(t_{n+1}) + \lambda u(t_{n+1}) + (u(t_{n+1})\cdot\nabla)u(t_{n+1}) \\
&+ \nabla p(t_{n+1}) = f^{n+1} + R_a g T(t_{n+1}) - R_s g C(t_{n+1}) + R_u^{n+1},
\end{aligned} \tag{18}
$$

$$
\frac{T(t_{n+1}) - T(t_n)}{\tau} - \chi_T\Delta T(t_{n+1}) + (u(t_{n+1})\cdot\nabla)T(t_{n+1}) = \gamma^{n+1} + R_T^{n+1}, \tag{19}
$$

$$
\begin{aligned}
&\frac{C(t_{n+1}) - C(t_n)}{\tau} - \chi_C\Delta C(t_{n+1}) + (u(t_{n+1})\cdot\nabla)C(t_{n+1}) + \kappa C(t_{n+1}) \\
&= \eta^{n+1} + R_C^{n+1} + \mathcal{L}\Psi(T(t_{n+1})),
\end{aligned} \tag{20}
$$

$$
\nabla\cdot u(t_{n+1}) = 0, \tag{21}
$$

where

$$R_u^{n+1} = \frac{1}{\tau}\int_{t_n}^{t_{n+1}} (t-t_n)u_{tt}(t)\mathrm{d}t, \quad R_T^{n+1} = \frac{1}{\tau}\int_{t_n}^{t_{n+1}} (t-t_n)T_{tt}(t)\mathrm{d}t,$$
$$R_C^{n+1} = \frac{1}{\tau}\int_{t_n}^{t_{n+1}} (t-t_n)C_{tt}(t)\mathrm{d}t.$$

Subtracting the first, second and third equations of (7) from (18), (19) and (20), respectively, it can be obtained

$$\begin{aligned}(22)\qquad &\frac{\widetilde{e}_u(t_{n+1}) - e_u(t_n)}{\tau} - \nu\Delta\widetilde{e}_u(t_{n+1}) + \lambda\widetilde{e}_u(t_{n+1})\\ &= [(u^n\cdot\nabla)\widetilde{u}^{n+1} - (u(t_{n+1})\cdot\nabla)u(t_{n+1})]\\ &\quad + \nu\nabla s^n - \nabla p(t_{n+1}) + R_a g e_T^{n+1} - R_s g e_C^{n+1} + R_u^{n+1},\end{aligned}$$

$$(23)\qquad \frac{e_T^{n+1}-e_T^n}{\tau} - \Delta e_T^{n+1} = [(u^n\cdot\nabla)T^{n+1} - (u(t_{n+1})\cdot\nabla)T(t_{n+1})] + R_T^{n+1},$$

$$\begin{aligned}(24)\qquad \frac{e_C^{n+1}-e_C^n}{\tau} - \Delta e_C^{n+1} + \kappa e_C^{n+1} &= [(u^n\cdot\nabla)C^{n+1} - (u(t_{n+1})\cdot\nabla)C(t_{n+1})]\\ &\quad + R_C^{n+1} + \mathcal{L}(\Psi(T(t_{n+1})) - \Psi(T^{n+1})).\end{aligned}$$

In addition, it can be concluded from (21) and Remark 3.1 that

$$(25)\qquad \nabla\cdot e_u^{n+1} = 0.$$

Taking the inner product of (22) with $2\tau\widetilde{e}_u^{n+1}$ and using Lemma 2.1 to have

$$\begin{aligned}(26)\qquad &\|\widetilde{e}_u^{n+1}\|_0^2 - \|e_u^n\|_0^2 + \|\widetilde{e}_u^{n+1} - e_u^n\|_0^2 + \lambda\|\widetilde{e}_u^{n+1}\|_0^2 + \nu\|\nabla\widetilde{e}_u^{n+1}\|_1^2\\ &= -2\tau b(u(t_{n+1}) - u(t_n), u(t_{n+1}), \widetilde{e}_u^{n+1}) - 2\tau b(e_u^n, u(t_{n+1}), \widetilde{e}_u^{n+1})\\ &\quad - 2\tau b(u^n, \widetilde{e}_u^{n+1}, \widetilde{e}_u^{n+1}) + 2\nu\tau(\nabla s^n, \widetilde{e}_u^{n+1}) - 2\tau(\nabla p(t_{n+1}), \widetilde{e}_u^{n+1})\\ &\quad + 2\tau(e_T^{n+1}, \widetilde{e}_u^{n+1}) + 2\tau(e_C^{n+1}, \widetilde{e}_u^{n+1}) + 2\tau(R_u^{n+1}, \widetilde{e}_u^{n+1}) = \sum_{n=1}^{8} B_i.\end{aligned}$$

According to (8) and (9), it can be derived that

$$(27)\qquad \|\widetilde{e}_u^{n+1}\|_0^2 = \|\nabla\rho^{n+1}\|_0^2 + \|e_u^{n+1}\|_0^2.$$

Now each term in the right hand side of (26) is bounded independently,

$$\begin{aligned}B_1 &= 2\tau b(u(t_{n+1}) - u(t_n), \widetilde{e}_u^{n+1}, u(t_{n+1}))\\ &\le c\tau\|u(t_{n+1}) - u(t_n)\|_0\|\nabla\widetilde{e}_u^{n+1}\|_0\|u(t_{n+1})\|_2\\ &\le c\tau\|\nabla\widetilde{e}_u^{n+1}\|_0\|\int_{t_n}^{t_{n+1}}|u_t|\mathrm{d}t\|_0 \le \frac{\tau\nu}{9}\|\nabla\widetilde{e}_u^{n+1}\|_0^2 + c\tau^2\int_{t_n}^{t_{n+1}}\|u_t\|_0^2\mathrm{d}t,\\ B_2 &= 2\tau b(e_u^n, \widetilde{e}_u^{n+1}, u(t_{n+1}))\\ &\le c\|e_u^n\|_0\|\nabla\widetilde{e}_u^{n+1}\|_0\|u(t_{n+1})\|_2 \le c\tau\|e_u^n\|_0^2 + \frac{\tau\nu}{9}\|\nabla\widetilde{e}_u^{n+1}\|_0^2,\end{aligned}$$

$$
\begin{aligned}
B_3 &= 2\tau b(u^n, \widetilde{e}_u^{n+1}, \widetilde{e}_u^{n+1}) = 0,\\
B_4 &= 2\nu\tau(\nabla s^n, \widetilde{e}_u^{n+1})\\
&= -2\nu\tau(s^n, \nabla\cdot(u(t_{n+1}) - \widetilde{u}^{n+1}))\\
&= 2\nu\tau(s^n, s^n - s^{n+1})\\
&\le c\tau(\|s^n\|_0^2 - \|s^{n+1}\|_0^2) + \frac{\tau\nu}{9}\|\nabla\widetilde{e}_u^{n+1}\|_0^2,\\
B_5 &= -2\tau(\nabla p(t_{n+1}), \widetilde{e}_u^{n+1})\\
&= 2\nu\tau(\nabla p(t_{n+1}), \nabla\rho^{n+1})\\
&\le c\tau\|\nabla p(t_{n+1})\|_0\|\nabla\rho^{n+1}\|_0 \le \|\nabla\rho^{n+1}\|_0^2 + c\tau^2\int_{t_n}^{t_{n+1}}\|\nabla p(t_{n+1})\|_0^2\mathrm{d}t,\\
B_6 &= 2\tau(e_T^{n+1}, \widetilde{e}_u^{n+1})\\
&\le \frac{\tau}{4}\|\nabla e_T^{n+1}\|_0^2 + \frac{\tau\nu}{9}\|\nabla\widetilde{e}_u^{n+1}\|_0^2,\\
B_7 &= 2\tau(e_C^{n+1}, \widetilde{e}_u^{n+1})\\
&\le \frac{\tau}{4}\|\nabla e_C^{n+1}\|_0^2 + \frac{\tau\nu}{9}\|\nabla\widetilde{e}_u^{n+1}\|_0^2,\\
B_8 &= 2\tau(R^{n+1}, \widetilde{e}_u^{n+1})\\
&\le c\tau^2\int_{t_n}^{t_{n+1}}\|u_{tt}\|_{-1}^2\mathrm{d}t + \frac{\tau\nu}{9}\|\nabla\widetilde{e}_u^{n+1}\|_0^2.
\end{aligned}
$$

Taking the inner product of (23), (24) in Step 1 with $2\tau e_T^{n+1}$ and $2\tau e_C^{n+1}$, separately, and using Lemma 2.1 to have

$$
\begin{aligned}
&\|e_T^{n+1}\|_0^2 - \|e_T^n\|_0^2 + \|e_T^{n+1} - e_T^n\|_0^2 + 2\tau\|\nabla e_T^{n+1}\|_0^2\\
&= 2\tau b(u(t_{n+1}) - u(t_n), T^{n+1}, e_T^{n+1}) + 2\tau b(e_u^n, T(t_{n+1}), e_T^{n+1})\\
&\quad - 2\tau b(u(t_{n+1}), e_T^{n+1}, e_T^{n+1}) + 2\tau(R_T^{n+1}, e_T^{n+1})\\
&= \sum_{n=1}^{4} D_i,
\end{aligned}
\tag{28}
$$

and

$$
\begin{aligned}
&\|e_C^{n+1}\|_0^2 - \|e_C^n\|_0^2 + \|e_C^{n+1} - e_C^n\|_0^2 + 2\tau\|\nabla e_C^{n+1}\|_0^2 + 2\kappa\tau\|e_C^{n+1}\|_0^2\\
&= 2\tau b(u(t_{n+1}) - u(t_n), C(t_{n+1}), e_C^{n+1}) + 2\tau b(e_u^n, C(t_{n+1}), e_C^{n+1})\\
&\quad - 2\tau b(u(t_{n+1}), e_C^{n+1}, e_C^{n+1}) + 2\tau(R_C^{n+1}, e_C^{n+1})\\
&\quad + 2\tau(\mathcal{L}(\Psi(T(t_{n+1})) - \Psi(T^{n+1})), e_C^{n+1}) = \sum_{n=1}^{5} E_i.
\end{aligned}
\tag{29}
$$

Using Young inequality, Cauchy inequalities and Sobolev imbedding theorems, it can be derived that

$$\begin{aligned}
D_1 &= 2\tau b(u(t_{n+1})-u(t_n),T(t_{n+1}),e_T^{n+1})\\
&\le c\tau\|u(t_{n+1})-u(t_n)\|_0\|\nabla e_T^{n+1}\|_0\|u(t_{n+1})\|_2\\
&\le c\tau\|\nabla e_T^{n+1}\|_0\|\int_{t_n}^{t_{n+1}}u_t\mathrm{d}t\|_0\le\frac{\tau}{5}\|\nabla e_T^{n+1}\|_0^2+c\tau^2\int_{t_n}^{t_{n+1}}\|u_t\|_0^2\mathrm{d}t,\\
D_2 &= 2\tau b(e_u^n,T(t_{n+1}),e_T^{n+1})\\
&\le c\tau\|e_u^n\|_0\|\nabla e_T^{n+1}\|_0\|T(t_{n+1})\|_2\\
&\le c\tau\|\nabla e_T^{n+1}\|_0\|\int_{t_n}^{t_{n+1}}u_t\mathrm{d}t\|_0\le\frac{\tau}{5}\|\nabla e_T^{n+1}\|_0^2+c\tau^2\int_{t_n}^{t_{n+1}}\|u_t\|_0^2\mathrm{d}t,\\
D_3 &= -2\tau b(u(t_{n+1}),e_T^{n+1},e_T^{n+1})=0,\\
D_4 &= 2\tau(R_T^{n+1},e_T^{n+1})\\
&\le\frac{\tau}{5}\|\nabla e_T^{n+1}\|_0^2+c\tau\|R_T^{n+1}\|_{-1}^2\le\frac{\tau}{5}\|\nabla e_T^{n+1}\|_0^2+c\tau^2\int_{t_n}^{t_{n+1}}\|T_{tt}\|_{-1}^2\mathrm{d}t.
\end{aligned}$$

Similarly

$$\begin{aligned}
E_1 &= 2\tau b(u(t_{n+1})-u(t_n),C(t_{n+1}),e_C^{n+1})\\
&\le c\tau\|\nabla e_C^{n+1}\|_0\|\int_{t_n}^{t_{n+1}}|u_t|\mathrm{d}t\|_0\le\frac{\tau}{5}\|\nabla e_C^{n+1}\|_0^2+c\tau^2\int_{t_n}^{t_{n+1}}\|u_t\|_0^2\mathrm{d}t,\\
E_2 &= 2\tau b(e_u^n,C(t_{n+1}),e_C^{n+1})\\
&\le c\tau\|e_u^n\|_0\|\nabla e_C^{n+1}\|_0\|C(t_{n+1})\|_2\\
&\le c\tau\|\nabla e_C^{n+1}\|_0\|\int_{t_n}^{t_{n+1}}|u_t|\mathrm{d}t\|_0\le\frac{\tau}{5}\|\nabla e_C^{n+1}\|_0^2+c\tau^2\int_{t_n}^{t_{n+1}}\|u_t\|_0^2\mathrm{d}t,\\
E_3 &= -2\tau b(u(t_{n+1}),e_C^{n+1},e_C^{n+1})=0,\\
E_4 &= 2\tau(R_C^{n+1},e_C^{n+1})\\
&\le\frac{\tau}{5}\|\nabla e_C^{n+1}\|_0^2+c\tau\|R_C^{n+1}\|_{-1}^2\le\frac{\tau}{5}\|\nabla e_C^{n+1}\|_0^2+c\tau^2\int_{t_n}^{t_{n+1}}\|C_{tt}\|_{-1}^2\mathrm{d}t,\\
E_5 &= 2\mathcal{L}\tau(\Psi(T(t_{n+1})-\Psi(T^{n+1}),e_C^{n+1})\\
&\le 2\mathcal{L}\tau\|T(t_{n+1})-T^{n+1}\|_0\|\nabla e_C^{n+1}\|_0\le c\tau\|\nabla e_T^{n+1}\|_0^2+\frac{\tau}{5}\|\nabla e_C^{n+1}\|_0^2,
\end{aligned}$$

from (26), (27), (28) and (29), it can be obtained

$$\begin{aligned}
(30)\quad &\|\widetilde{e}_u^{n+1}\|_0^2-\|e_u^n\|_0^2+\|\widetilde{e}_u^{n+1}-e_u^n\|_0^2+\nu\tau\|\nabla\widetilde{e}_u^{n+1}\|_1^2+\nu\tau(\|s^{n+1}\|_0^2-\|s^n\|_0^2)\\
&+\|e_T^{n+1}\|_0^2-\|e_T^n\|_0^2+\|e_C^{n+1}-e_T^n\|_0^2+c\tau\|\nabla e_T^{n+1}\|_0^2\\
&+\|e_C^{n+1}\|_0^2-\|e_C^n\|_0^2+\|e_C^{n+1}-e_C^n\|_0^2+c\tau\|\nabla e_C^{n+1}\|_0^2
\end{aligned}$$

$$\leq c\tau^2 \int_{t_n}^{t_{n+1}} (\|\nabla p(t)\|_0^2 + \|u_t\|_0^2 + \|u_{tt}\|_{-1}^2 + \|T_{tt}\|_{-1}^2 + \|C_{tt}\|_{-1}^2)\mathrm{d}t + c\tau\|e_u^n\|_0^2.$$

Summing up (30) $n = 0, 1, \ldots, N-1$, and using the regularity properties, stability and applying Lemma 2.1, then the proof is finished. □

Theorem 3.4. *Suppose Assumption 1, Assumption 2 hold. Then for all* $N = 1, 2, \ldots, \mathcal{N} - 1$, *there exists*

$$\tau \sum_{n=0}^{N} \|p(t_{n+1}) - p^{n+1}\|_0^2 \leq c\tau. \tag{31}$$

Proof. By substituting (10) into the first equation of (7), it can be obtained

$$\begin{aligned} &\frac{u^{n+1} - u^n}{\tau} - \nu\Delta\widetilde{u}^{n+1} + (u^n \cdot \nabla)\widetilde{e}_u^{n+1} + \nabla p^{n+1} - \nu(\nabla s^n - \nabla s^{n+1}) \\ &= f^{n+1} + R_a T^{n+1} - R_s C^{n+1}. \end{aligned} \tag{32}$$

Now subtract (32) from (18), which can be obtained

$$\begin{aligned} &\frac{e_u^{n+1} - e_u^n}{\tau} + \nu\Delta\widetilde{e}_u^{n+1} + \nabla e_p^{n+1} \\ &= [(u^n \cdot \nabla)\widetilde{u}^{n+1} - (u(t_{n+1}) \cdot \nabla)u(t_{n+1})] - \nu(\nabla s^{n+1} - \nabla s^n) \\ &\quad + R_a e_T^{n+1} - R_s e_C^{n+1} + R_u^{n+1}. \end{aligned} \tag{33}$$

Taking the inner product of (33) with $v \in H_0^1(\Omega)$, it can be derived that

$$(e_p^{n+1}, \nabla \cdot v) = \sum_{1}^{7} K_i, \tag{34}$$

where

$$\begin{aligned} K_1 &= (\frac{\|e_u^n - e_u^{n+1}\|_0}{\tau}, v) \leq c\tau\|e_u^n - e_u^{n+1}\|_0\|\nabla v\|_0, \\ K_2 &= \nu(\Delta\widetilde{e}_u^{n+1}, v) \leq c\nu\|\nabla\widetilde{e}_u^{n+1}\|_0\|\nabla v\|_0, \\ K_3 &= (u(t_{n+1} - u(t_n) + e_u^n, u(t_{n+1}), v) + (u(t_n) - e_u^n, \widetilde{e}_u^{n+1}, v) \\ &\leq (\|u(t_{n+1}) - u(t_n)\|_0 + \|e_u^n\|_0)\|u(t_{n+1})\|_2\|\nabla v\|_0 \\ &\quad + (\|u(t_n)\|_1 + \|e_u^n\|_1)\|\widetilde{e}_u^{n+1}\|_0\|\nabla v\|_0, \\ K_4 &= \nu(s^{n+1} - s^n, \nabla \cdot v) = \nu(\nabla \cdot \widetilde{e}_u^{n+1}, \nabla \cdot v) \\ &\leq c\nu\|\nabla\widetilde{e}_u^{n+1}\|_0\|\nabla v\|_0, \\ K_5 &= R_a(e_T^{n+1}, v) \leq c\|e_T^{n+1}\|_0\|\nabla v\|_0, \\ K_6 &= -R_s(e_C^{n+1}, v) \leq c\|e_C^{n+1}\|_0\|\nabla v\|_0, \\ K_7 &= (R_u^{n+1}, v) \leq c\tau\|u_{tt}\|_{-1}\|\nabla v\|_0. \end{aligned}$$

Combining the above inequalities, it can be obtained that

$$\beta\|e_p^{n+1}\|_0 \le c(\frac{1}{\tau}\|e_u^n - e_u^{n+1}\|_0 + \nu\|\nabla\widetilde{e}_u^{n+1}\|_0 + \tau\|u_{tt}\|_{-1}) + c(\|u(t_{n+1}) - u(t_n)\|_0 + \|e_u^n\|_0). \tag{35}$$

According to the conclusion above, the proof of (31) is finished. □

4. Fully discrete Gauge-Uzawa scheme

In this section, the first-order scheme of the Gauge-Uzawa methods for the DBTC are introduced. Let $\mathcal{K}_h = \{K\}$ be a uniformly regular family of triangulation of Ω and define the mesh size $h = \max\limits_{K\in\mathcal{K}_h}\{\mathrm{diam}(K)\}$. The spatial approximation of velocity, pressure, temperature and salt concentration are applied by mixed element method with $(X_h, Y_h, M_h, M_h) \subset (X, Y, M, M)$. The following discrete subspaces are defined:

$$X_h = \Big\{v_h \in X \cap \mathcal{C}^0(\Omega)^d : v_h|_K \in [P_1(K) \oplus span\,\{b\}]^d, \forall K \in \mathcal{K}_h\Big\},$$
$$Y_h = \Big\{q_h \in Y \cap \mathcal{C}^0(\Omega) : q_h|_K \in P_1(K), \forall K \in \mathcal{K}_h\Big\},$$
$$M_h = \Big\{s_h \in Y \cap \mathcal{C}^0(\Omega) : s_h|_K \in P_1(K), \forall K \in \mathcal{K}_h\Big\}.$$

The first order fully discrete Gauge-Uzawa scheme is as follows:

Algorithm 2: Suppose u_h^0, T_h^0, C_h^0 are given and let $s_h^0 = 0$, assume that u_h^n, T_h^n and C_h^n are known, for all $v_h \in X_h$, ψ_h and $q_h \in Y_h$, $z_h \in M_h$. Then find $\widetilde{u}_h^{n+1}$, u_h^{n+1}, p_h^{n+1}, T_h^{n+1}, C_h^{n+1} from the following steps:

Step 1. Find $\widetilde{u}_h^{n+1}$, T_h^{n+1} and C_h^{n+1} as the solution of

$$\begin{cases} (\frac{\widetilde{u}_h^{n+1}-u_h^n}{\tau}, v_h) + \nu(\nabla\widetilde{u}_h^{n+1}, \nabla v_h) + \lambda(\widetilde{u}_h^{n+1}, v_h) + ((u_h^n\cdot\nabla)\widetilde{u}_h^{n+1}, v_h) \\ = (f^{n+1}, v_h) + (R_a g T_h^{n+1}, v_h) - (R_s g C^{n+1}, v_h) + \nu(s_h^n, \nabla\cdot v_h), \\ (\frac{T_h^{n+1}-T_h^n}{\tau}, z_h) + (\nabla T_h^{n+1}, \nabla z_h) + ((u_h^n\cdot\nabla)T_h^{n+1}, z_h) = (\gamma^{n+1}, z_h), \\ (\frac{C_h^{n+1}-C_h^n}{\tau}, z_h) + (\nabla C_h^{n+1}, \nabla z_h) + ((u_h^n\cdot\nabla)C_h^{n+1}, z_h) \\ = (\eta^{n+1}, z_h) + (\mathcal{L}\Psi(T_h^{n+1}), z_h) - (\kappa C_h^{n+1}, z_h), \\ \widetilde{u}_h^{n+1}|_{\partial\Omega} = 0, \quad T_h^{n+1}|_{\partial\Omega} = 0, \quad C_h^{n+1}|_{\partial\Omega} = 0. \end{cases} \tag{36}$$

Step 2. Find ρ_h^{n+1} as the solution of

$$(\nabla\rho_h^{n+1}, \nabla\psi_h) = (\nabla\cdot\widetilde{u}_h^{n+1}, \nabla\psi_h). \tag{37}$$

Step 3. Update u_h^{n+1}, s_h^{n+1} by

$$\begin{cases} u_h^{n+1} = \widetilde{u}_h^{n+1} + \nabla\rho_h^{n+1}, \\ (s_h^{n+1}, q_h) = (s_h^n, q_h) - (\nabla\cdot\widetilde{u}_h^{n+1}, q_h). \end{cases} \tag{38}$$

Step 4. Update p_h^{n+1} by

$$p_h^{n+1} = -\frac{1}{\tau}\rho_h^{n+1} + \nu s_h^{n+1}. \tag{39}$$

Theorem 4.1. *For all $1 \le N \le \mathcal{N}-1$, the numerical solution of Algorithm 2 is unconditionally stable*

$$
\begin{aligned}
(40)\qquad & \|\widetilde{u}_h^N\|_0^2 + \|T_h^N\|_0^2 + \|C_h^N\|_0^2 + \nu\tau\|s_h^N\|_0^2 \\
& + \sum_{n=0}^{N-1}(\|\widetilde{u}_h^{n+1} - u_h^n\|_0^2 + \|T_h^{n+1} - T_h^n\|_0^2 + \|C_h^{n+1} - C_h^n\|_0^2) \\
& + \tau\sum_{n=0}^{N-1}(\nu\|\nabla\widetilde{u}_h^{n+1}\|_0^2 + \|\nabla T_h^{n+1}\|_0^2 + \|\nabla C_h^{n+1}\|_0^2) \\
\le\ & \|u_h^0\|_0^2 + \|T_h^0\|_0^2 + \|C_h^0\|_0^2 + \nu\tau\|s_h^0\|_0^2 \\
& + c\int_0^{\mathcal{T}}(\|f(t)\|_0^2 + \|\gamma(t)\|_0^2 + \|\eta(t)\|_0^2)\mathrm{d}t + c\tau\mathcal{L}.
\end{aligned}
$$

Proof. Taking the inner product of (36) with $2\tau\widetilde{u}_h^{n+1}$, $2\tau T_h^{n+1}$ and $2\tau C_h^{n+1}$ to have

$$
(41)\quad \begin{cases}
\|T_h^{n+1}\|_0^2 - \|T_h^n\|_0^2 + \|T_h^{n+1} - T_h^n\|_0^2 + 2\tau\|\nabla T_h^{n+1}\|_0^2 \\
= 2\tau(\gamma^{n+1}, T_h^{n+1}) \\
\le 2\tau\|T_h^{n+1}\|_0\|\gamma^{n+1}\|_0 \\
\le \dfrac{\tau}{2}\|\nabla T_h^{n+1}\|_0^2 + c\displaystyle\int_{t_n}^{t_{n+1}}\|\gamma(t)\|_0^2\mathrm{d}t, \\
\|C_h^{n+1}\|_0^2 - \|C_h^n\|_0^2 + \|C_h^{n+1} - C_h^n\|_0^2 + 2\tau\|\nabla C_h^{n+1}\|_0^2 + 2\kappa\tau\|C_h^{n+1}\|_0^2 \\
= 2\tau(\eta^{n+1}, C_h^{n+1}) + 2\tau(\mathcal{L}\Psi(T_h^{n+1}), C_h^{n+1}) \\
\le \dfrac{\tau}{2}\|\nabla C_h^{n+1}\|_0^2 + c\tau\mathcal{L} + c\displaystyle\int_{t_n}^{t_{n+1}}\|\eta(t)\|_0^2\mathrm{d}t,
\end{cases}
$$

$$
\begin{aligned}
(42)\qquad & \|\widetilde{u}_h^{n+1}\|_0^2 - \|u_h^n\|_0^2 + \|\widetilde{u}_h^{n+1} - u_h^n\|_0^2 \\
& + 2\tau\|\nabla\widetilde{u}_h^{n+1}\|_0^2 + 2\tau\lambda\|\widetilde{u}_h^{n+1}\|_0^2 + 2\tau(\nabla s_h^n, \widetilde{u}_h^{n+1}) \\
= {} & 2\tau(f^{n+1}, \widetilde{u}_h^{n+1}) + 2\tau R_a(T_h^{n+1}, \widetilde{u}_h^{n+1}) - 2\tau R_s(C_h^{n+1}, \widetilde{u}_h^{n+1}).
\end{aligned}
$$

It can be obtained from (37) and (38) that

$$
\begin{aligned}
(43)\qquad \|u_h^n\|_0^2 &= (u_h^n, u_h^n) = (\widetilde{u}_h^n + \nabla\rho_h^n, u_h^n) \\
&= (\widetilde{u}_h^n, u_h^n) = (\widetilde{u}_h^n, \widetilde{u}_h^n + \nabla\rho_h^n) = \|\widetilde{u}_h^n\|_0^2 - \|\nabla\rho_h^n\|_0^2.
\end{aligned}
$$

So (42) becomes

$$
\begin{aligned}
(44)\qquad & \|\widetilde{u}_h^{n+1}\|_0^2 - \|\widetilde{u}_h^n\|_0^2 + \|\widetilde{u}_h^{n+1} - u_h^n\|_0^2 \\
& + 2\tau\|\nabla\widetilde{u}_h^{n+1}\|_0^2 + 2\tau\lambda\|\widetilde{u}_h^{n+1}\|_0^2 + \|\nabla\rho_h^n\|_0^2 \\
= {} & 2\tau(f^{n+1}, \widetilde{u}_h^{n+1}) + 2\tau Ra(T_h^{n+1}, \widetilde{u}_h^{n+1})
\end{aligned}
$$

$$-2\tau Rs(C_h^{n+1},\widetilde{u}_h^{n+1})+2\tau(s_h^n,\nabla\cdot\widetilde{u}_h^{n+1})=\sum_{n=1}^{4}F_i.$$

From the Cauchy-Schwarz inequality and (9), there exists

$$\begin{aligned}
F_1&=2\nu\tau(s_h^n,s_h^{n+1}-s_h^n)\\
&=-\nu\tau(\|s_h^{n+1}\|_0^2-\|s_h^n-s_h^{n+1}\|_0^2-\|s_h^n\|_0^2)\\
&\le-\nu\tau(\|s_h^{n+1}\|_0^2-\|s_h^n\|_0^2)+\nu\tau\|\nabla\widetilde{u}_h^{n+1}\|_0^2,\\
F_2&=2\tau(f^{n+1},\widetilde{u}_h^{n+1})\\
&\le2\tau\|f^{n+1}\|_0\|\widetilde{u}_h^{n+1}\|_0\\
&\le\frac{\nu\tau}{4}\|\widetilde{u}_h^{n+1}\|_0^2+c\int_{t_n}^{t_{n+1}}\|f(t)\|_0^2\mathrm{d}t,\\
F_3&=2\tau(RaT_h^{n+1},\widetilde{u}_h^{n+1})\\
&\le\frac{\nu\tau}{4}\|\widetilde{u}_h^{n+1}\|_0^2+\frac{\tau}{2}\|\nabla T_h^{n+1}\|_0^2,\\
F_4&=-2\tau(RsC_h^{n+1},\widetilde{u}_h^{n+1})\\
&\le\frac{\nu\tau}{4}\|\widetilde{u}_h^{n+1}\|_0^2+\frac{\tau}{2}\|\nabla C_h^{n+1}\|_0^2.
\end{aligned}$$

Adding (40) and (41), then sum up $n=0,1,\ldots,N-1$, the proof of (40) is finished. □

5. Numerical experiments

In this section, some numerical experiments are implemented to verify the accuracy of the Gauge-Uzawa methods for the DBTC. In the numerical experiments, all computational domain are set as $\Omega=[0,1]^d$. And the P_1b-P_1-P_1-P_1 finite element pairs are selected to approximate the velocity, pressure, temperature and salt concentration, respectively. All the numerical experiments are implemented by using the public domain finite element software FreeFEM++ [6].

5.1. Convergence rate verification

In this subsection, the following symbols are used to denote the relative errors in the tables.

$$\begin{aligned}
&E_0^{u,h}=\frac{\|u-u_h\|_0}{\|u\|_0},\ E_1^{u,h}=\frac{\|u-u_h\|_1}{\|u\|_1},\ E_0^{p,h}=\frac{\|p-p_h\|_0}{\|p\|_0},\\
&E_0^{T,h}=\frac{\|T-T_h\|_0}{\|T\|_0},\ E_1^{T,h}=\frac{\|T-T_h\|_1}{\|T\|_1},\ E_0^{C,h}=\frac{\|C-C_h\|_0}{\|C\|_0},\\
&E_1^{C,h}=\frac{\|C-C_h\|_1}{\|C\|_1}.
\end{aligned}$$

In the following experiment, the following physical parameters are set, $\lambda = Rs = Ra = \kappa = \mathcal{L} = 1$. In the 2D case, the problem with the following analytical solutions are considered,

$$\begin{aligned}(u_1, u_2) &= (-\sin(\pi y)\sin^2(\pi x)\cos(\pi y)\sin(t), \sin(\pi x)\sin^2(\pi y)\cos(\pi x)\sin(t)),\\ p &= \cos(\pi y)\sin(\pi x)\sin(t),\\ T &= (-\sin(\pi y)\sin^2(\pi x)\cos(\pi y) + \sin(\pi x)\sin^2(\pi y)\cos(\pi x))\sin(t),\\ C &= (-\cos(\pi y)\sin^2(\pi x)\sin(\pi y) - \cos(\pi x)\sin(\pi x)\sin^2(\pi y))\sin(t).\end{aligned}$$

TABLE 1. The Gauge-Uzawa method for 2D DBTC

$\frac{1}{h}$	$E_0^{u,h}$	$rate$	$E_1^{u,h}$	$rate$	$E_0^{p,h}$	$rate$	$E_0^{T,h}$	$rate$	$E_1^{T,h}$	$rate$	$E_0^{C,h}$	$rate$	$E_1^{C,h}$	$rate$
4	3.91E-01	0	5.60E-01	0	1.51E-00	0	3.42E-01	0	4.63E-01	0	5.68E-01	0	6.97E-01	0
8	1.25E-01	1.64	3.01E-02	0.90	0.61E-01	1.30	0.10E-01	1.78	2.30E-01	1.01	0.21E-01	1.43	3.87E-01	0.85
16	3.28E-02	1.93	1.52E-01	0.99	2.00E-01	1.61	2.59E-02	1.95	1.14E-01	1.01	5.90E-02	1.84	1.96E-01	0.98
32	8.28E-03	1.99	7.58E-02	1.00	6.70E-02	1.58	6053E-03	1.99	5.67E-02	1.00	1.52E-04	1.96	9.81E-02	1.00
64	2.08E-03	2.00	3.78E-02	1.00	2.31E-02	1.53	1.63E-03	2.00	2.83E-02	1.00	3.82E-03	1.99	4.91E-02	1.00
128	5.21E-04	2.00	1.89E-02	1.00	8.11E-03	1.51	4.10E-04	2.00	1.42E-02	1.00	9.59E-04	2.00	2.46E-02	1.00

Similarly, in the 3D case, the problem with the following analytical solutions are considered,

$$\begin{aligned}(u_1, u_2, u_3) &= ((y^4 + z^2)\cos(t), (z^4 + x^2)\cos(t), (x^4 + y^2)\cos(t)),\\ p &= (2x - 1)(2y - 1)(2z - 1)\cos(t),\\ T &= (0.5 + 0.5\cos(xyz))\cos(t),\\ C &= (0.3 + 0.3e^{xyz})\cos(t).\end{aligned}$$

TABLE 2. The Gauge-Uzawa method for 3D DBTC

$\frac{1}{h}$	$E_1^{u,h}$	$rate$	$E_0^{u,h}$	$rate$	$E_0^{p,h}$	$rate$	$E_0^{T,h}$	$rate$	$E_1^{T,h}$	$rate$	$E_0^{C,h}$	$rate$	$E_1^{C,h}$	$rate$
4	2.08E-01		5.70E-02		1.11E-00		3.66E-03		5.30E-01		8.41E-03		3.86E-01	
8	1.05E-01	0.98	1.45E-02	1.98	5.18E-00	1.11	9.16E-04	2.00	2.63E-01	1.00	2.03E-03	2.05	1.91E-01	1.02
12	7.02E-02	1.00	6.43E-03	2.00	2.65E-01	1.65	4.07E-04	2.00	1.75E-01	1.00	8.94E-04	2.02	1.27E-01	1.00
16	5.27E-02	1.00	3.62E-02	2.00	1.70E-01	1.54	2.29E-04	2.00	1.31E-01	1.00	5.01E-04	2.01	9.52E-02	1.01

The numerical results are listed in Table 1 and Table 2. It can be seen that the presented method can get a linear convergence rate for the computed velocity, temperature and salt concentration in the $H^1(\Omega)^d$ semi-norm, and about 1.5 convergence order for the computed pressure in the $L^2(\Omega)$ norm. Moreover, it is easy to see that a quadratic convergence rate both for the computed velocity, temperature and salt concentration in the $L^2(\Omega)$ norm, which verifies the theoretical results.

5.2. The porous cavity problem

Figure 1 shows the computational domain with boundary conditions. The Dirichlet boundary conditions are considered for the presented method, its are still valid for Neumann boundary conditions. The no-slip boundary conditions are imposed for the velocity. The upper and lower boundary conditions of temperature and salt concentration are $\partial T/\partial n = 0$ and $\partial C/\partial n = 0$. The temperature and salt concentration are kept at T_R, C_R for right and T_L, C_L for left vertical walls with $T_R < T_L$, $C_R < C_L$, respectively. $T_R = C_R = -1$ and $T_L = C_L = 1$ are considered.

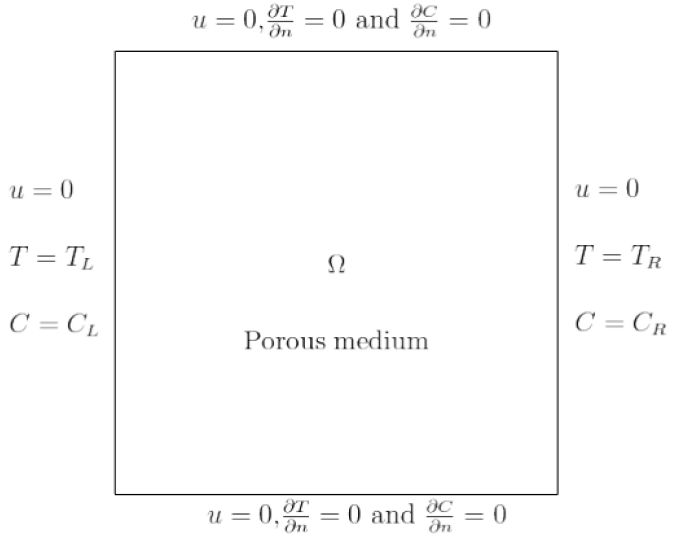

FIGURE 1. The schematic diagram of the computational domain with its boundary conditions.

In Figure 2, $\mathcal{L}\Psi(T) = \mathcal{L}T$ is considered. The isolines of temperature, salt concentration, pressure, and arrow plot of velocity for $\lambda = 10^3$, $Rs = 10$, at $\mathcal{L}$=1, 10, and 100, are drawn respectively. It can be easily seen from Figure 2. As the chemical equilibrium coefficient increases, the effect of temperature on salt concentration becomes obvious, and the upper part of the square cavity has a high concentration, but has little effect on velocity, pressure and temperature.

5.3. The partitioned square enclosure problem

In order to verify the effectiveness of the method, the partitioned square enclosure problem is tested. This experiment is an important practical problem,

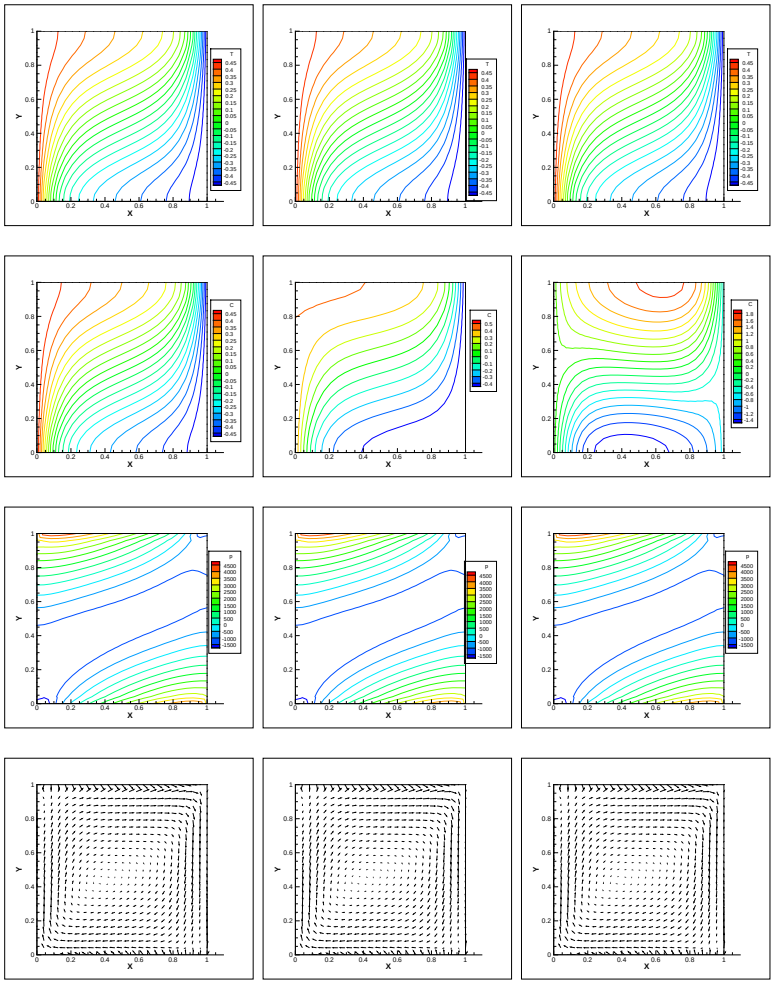

FIGURE 2. Isolines of temperature, salt concentration, pressure and arrow plot of velocity for $\lambda = 10^3$, $Ra = 10^3$, $Rs = 10$, at $\mathcal{L} = 1, 10, 10^2$, from top to bottom.

which has been investigated in [3, 7]. The geometry and the boundary conditions are that left and right walls are kept at $T_L = C_L = 0$ and $T_R = C_R = 1$, respectively. The remaining walls are kept $\partial T/\partial n = \partial C/\partial n = 0$. And there are two rectangular insulators in this square cavity. Though its geometry and boundary conditions are simple, it has characteristics of a very complex flow which occurs in many practical engineering applications.

The length and thickness of the insulators to 0.25 and 0.1 are set, respectively. And considering three different placement locations. The first placement of $x = 0.5$. Further, in the other two placed mode, the insulators are offset to the left $x = 0.25$ or at the right $x = 0.75$. At this point $\mathcal{L} = 1$, $Rs = 10$, $\lambda = 10^3$, $Ra = 10^3$. Figure 3 shows that the arrow plot of velocity, the contour lines of pressure, temperature and salt concentration.

Figure 3 shows that there is a vortex in the partition-hot wall region for the left partition and in the partition-cold wall region for the right partition, respectively. For the intermediate partition two small vortices can be found. Moreover, for the left partition, the flow coming off the hot wall is cooled by the perfectly conducting end wall and the partition. For the right partition, the heated flow is confined to the partition-hot wall region, because of the heated flow moving up the hot wall and the cooled flow moving down the hot wall.

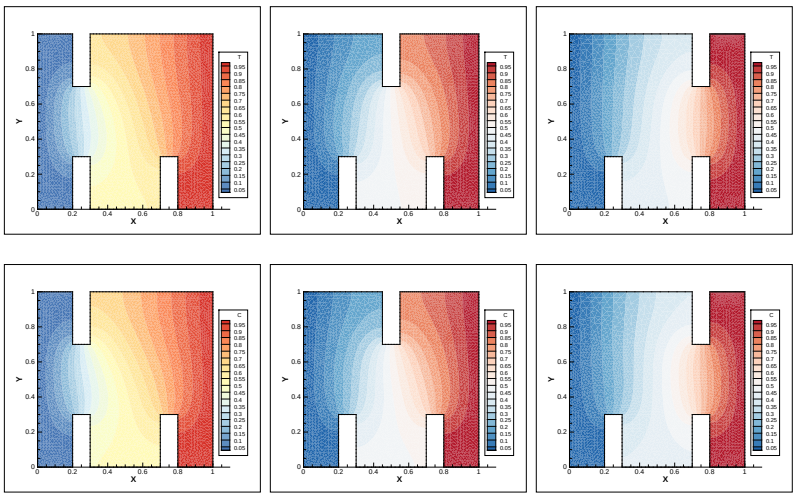

5.4. A square enclosure with a circular cylinder problem

The final experiment is an important practical problem. In many engineering applications, especially in relation to heat losses from thermal storage systems such as solar collectors, nuclear reactor design, buildings and aircraft cabin insulation, the problem is researched to find means to improve the insulating properties of fluid layers. The computational domain consists of a square enclosure with sides of length 1, within which two circular cylinders with radius 0.1 are located in the center of the square cavity. The cylinders are kept at high temperature and salt concentration of T_{in} and C_{in}, while the walls of the square enclosure are kept at low temperature and salt concentration of T_{out} and C_{out}. Let $T_{in} = C_{in} = 0.5$, $T_{out} = C_{out} = -0.5$. Besides, no-slip boundary conditions for the velocity on the whole boundary are imposed.

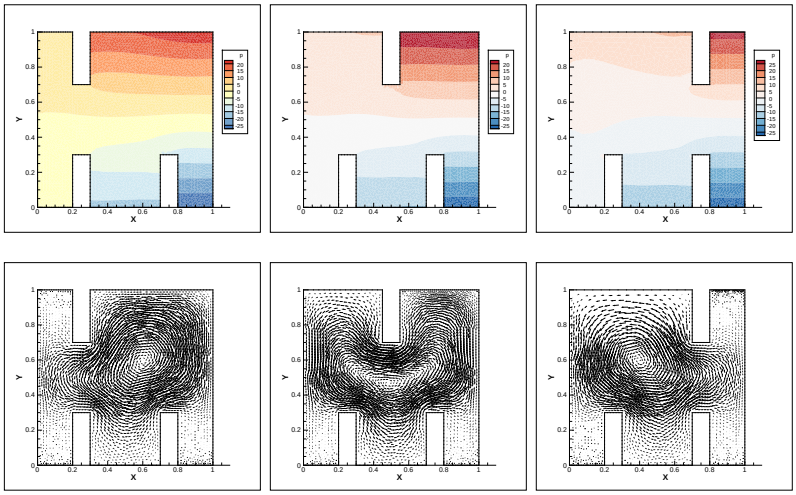

FIGURE 3. Contour lines of temperature, salt concentration, pressure, and arrow plot of velocity for $\lambda = 10^3$, $Rs = 10$, $A = 1$ at $Ra = 10^3$, $\mathcal{L} = 1$ from top to bottom.

In this test, $\lambda = 10^2$, 10^3, 10^4 and the other parameters $Rs = 10$, $Ra = 10^4$ are set. As seen from Figure 4, the arrow plot of velocity, contour lines of temperature and salt concentration in the square cavity are always symmetric, due to the boundary conditions. When $\lambda = 10^4$, two vortices appear on the right side and left side of the cavity, respectively. Because of the difference of the temperature and salt concentration, the left vortex and the right one behave a counterclockwise recirculation and a clockwise recirculation, respectively. Moreover, with the decrease of the value of λ, the permeability increases and the resistance of the medium to the fluid decreases, which leads to these vortices moving toward the top wall of the square cavity.

6. Conclusions

In this paper the Gauge-Uzawa methods are presented for the DBTC. In the view of theoretical analysis, the presented methods only need to solve linear, decoupled elliptic equations at each time. It is proved that first order semi-discrete Gauge-Uzawa method is unconditionally stable and the error estimations of velocity, temperature and salt concentration are given. Furthermore, the unconditionally stability of the first order fully discrete Gauge-Uzawa method is deduced. Numerical experiments show that the Gauge-Uzawa methods are effective and the methods can also be used to simulate a simplified porous cavity problem. There still need some more theoretical analysis and modification to extend the presented methods to other concrete problems.

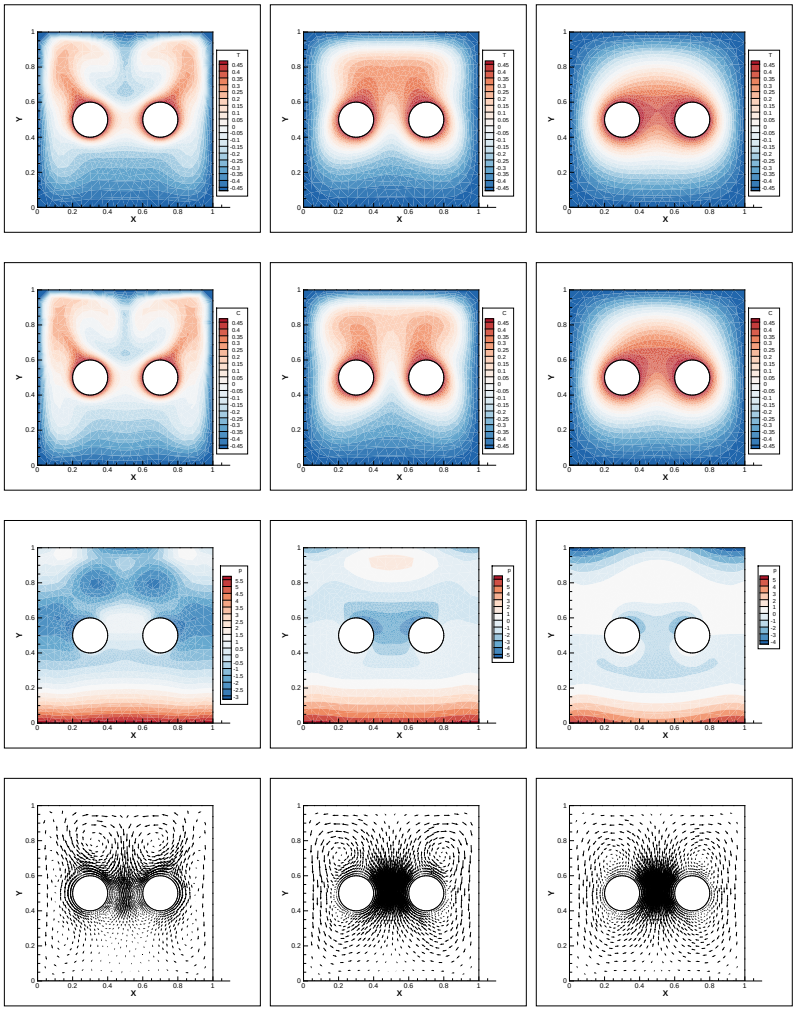

FIGURE 4. Contour lines of temperature, salt concentration, pressure and arrow plot of velocity (from top to bottom) with $\lambda = 10^2$, $\lambda = 10^3$, and $\lambda = 10^4$ (from left to right), at $Ra = 10^4$, $\mathcal{L} = 1$.

References

[1] M. T. Balhoff, A. Mikelić, and M. F. Wheeler, *Polynomial filtration laws for low Reynolds number flows through porous media*, Transp. Porous Media **81** (2010), no. 1, 35–60. https://doi.org/10.1007/s11242-009-9388-z

[2] A. B. Çıbık, M. Demir, and S. Kaya, *A family of second order time stepping methods for the Darcy-Brinkman equations*, J. Math. Anal. Appl. **472** (2019), no. 1, 148–175. https://doi.org/10.1016/j.jmaa.2018.11.015

[3] E. Ghasemi, S. Soleimani, and H. Bararnia, *Natural convection between a circular enclosure and an elliptic cylinder using control volume based finite element method*, Int. Commun. Heat Mass Transf. **39** (2012), no. 8, 1035–1044.

[4] B. Goyeau and J. Songbe, *Numerical study of double-diffusive natural convection in a porous cavity using the Darcy-Brinkman formulation*, Int. J. Heat Mass Transf. **39** (1996), no. 7, 1363–1378.

[5] B. Goyeau, J. Songbe, and D. Gobin, *Numerical study of double-diffusive natural convection in a porous cavity using the Darcy-Brinkman formulation*, Int. J. Heat Mass Transf. **39** (1996), no. 3, 1363–1378.

[6] F. Hecht, *New development in freefem++*, J. Numer. Math. **20** (2012), no. 3-4, 251–265. https://doi.org/10.1515/jnum-2012-0013

[7] B. S. Kim, D. S. Lee, M. Y. Ha, and H. S. Yoon, *A numerical study of natural convection in a square enclosure with a circular cylinder at different vertical locations*, Int. J. Heat Mass Transf. **51** (2007), no. 7, 1888–1906.

[8] C. Liao and P. Huang, *The modified characteristics finite element method for time-dependent Darcy-Brinkman problem*, Eng. Comput. **36** (2019), no. 1, 356–376.

[9] Y. Liu, *Convergence and continuous dependence for the Brinkman-Forchheimer equations*, Math. Comput. Modelling **49** (2009), no. 7-8, 1401–1415. https://doi.org/10.1016/j.mcm.2008.11.010

[10] M. S. Malashetty and B. S. Biradar, *The onset of double diffusive reaction-convection in an anisotropic porous layer*, Phys. Fluids **23** (2011), no.6, 64–102.

[11] R. H. Nochetto and J.-H. Pyo, *The gauge-Uzawa finite element method. I. The Navier-Stokes equations*, SIAM J. Numer. Anal. **43** (2005), no. 3, 1043–1068. https://doi.org/10.1137/040609756

[12] R. H. Nochetto and J.-H. Pyo, *The gauge-Uzawa finite element method. II. The Boussinesq equations*, Math. Models Methods Appl. Sci. **16** (2006), no. 10, 1599–1626. https://doi.org/10.1142/S0218202506001649

[13] D. Pritchard and C. N. Richardson, *The effect of temperature-dependent solubility on the onset of thermosolutal convection in a horizontal porous layer*, J. Fluid Mech. **571** (2007), 59–95. https://doi.org/10.1017/S0022112006003211

[14] J.-H. Pyo, *Optimal error estimate for semi-discrete gauge-Uzawa method for the Navier-Stokes equations*, Bull. Korean Math. Soc. **46** (2009), no. 4, 627–644. https://doi.org/10.4134/BKMS.2009.46.4.627

[15] J.-H. Pyo, *Error estimates for the second order semi-discrete stabilized gauge-Uzawa method for the Navier-Stokes equations*, Int. J. Numer. Anal. Model. **10** (2013), no. 1, 24–41.

[16] J.-H. Pyo and J. Shen, *Gauge-Uzawa methods for incompressible flows with variable density*, J. Comput. Phys. **221** (2007), no. 1, 181–197. https://doi.org/10.1016/j.jcp.2006.06.013

[17] Y. Ren and D. Liu, *Pressure correction projection finite element method for the 2D/3D time-dependent thermomicropolar fluid problem*, Comput. Math. Appl. **136** (2023), 136–150. https://doi.org/10.1016/j.camwa.2023.02.011

[18] Q. Shao, M. Fahs, and A. Younes, *A high-accurate solution for Darcy-Brinkman double-diffusive convection in saturated porous media*, Numer. Heat Transf. B: Fundam. **69** (2016), no. 1, 26–47.

[19] J. Shen, *On error estimates of projection methods for Navier-Stokes equations: first-order schemes*, SIAM J. Numer. Anal. **29** (1992), no. 1, 57–77. https://doi.org/10.1137/0729004

[20] R. M. Temam, *Navier-Stokes equations*, third edition, Studies in Mathematics and its Applications, 2, North-Holland, Amsterdam, 1984.

[21] F. Tone, X. M. Wang, and D. Wirosoetisno, *Long-time dynamics of* 2*d double-diffusive convection*: *analysis and/of numerics*, Numer. Math. **130** (2015), no. 3, 541–566. https://doi.org/10.1007/s00211-014-0670-9

[22] S. Wang and W. Tan, *The onset of Darcy-Brinkman thermosolutal convection in a horizontal porous media*, Phys. Lett. A **373** (2009), no. 7, 776–780.

[23] J. Wu, J. Shen, and X. Feng, *Unconditionally stable gauge-Uzawa finite element schemes for incompressible natural convection problems with variable density*, J. Comput. Phys. **348** (2017), 776–789. https://doi.org/10.1016/j.jcp.2017.07.045

[24] Y.-B. Yang and Y. L. Jiang, *An explicitly uncoupled VMS stabilization finite element method for the time-dependent Darcy-Brinkman equations in double-diffusive convection*, Numer. Algorithms **78** (2018), no. 2, 569–597. https://doi.org/10.1007/s11075-017-0389-7

[25] Y. Zeng, P. Z. Huang, and Y. He, *Deferred defect-correction finite element method for the Darcy-Brinkman model*, ZAMM Z. Angew. Math. Mech. **101** (2021), no. 11, Paper No. e202000285, 37 pp. https://doi.org/10.1002/zamm.202000285

[26] W. Zhu, P. Z. Huang, and K. Wang, *Newton iterative method based on finite element discretization for the stationary Darcy-Brinkman equations*, Comput. Math. Appl. **80** (2020), no. 12, 3098–3122. https://doi.org/10.1016/j.camwa.2020.10.020

Yangwei Liao
College of Mathematics and System Science
Xinjiang University
Urumqi 830046, P. R. China
Email address: liaoyangwei@stu.xju.edu.cn

Demin Liu
College of Mathematics and System Science
Xinjiang University
Urumqi 830046, P. R. China
Email address: followtime@126.com, mathldm@xju.edu.cn